# Underwater Direction of Arrival Estimation using Wideband Arrays of Opportunity

Elizaveta Dubrovinskaya[♯‡] and Paolo Casari[♯]

[♯]IMDEA Networks Institute, Madrid, Spain [‡]University Carlos III of Madrid, Spain

***Abstract*—We present a scheme to estimate the direction of arrival of acoustic signals reflected by underwater targets using wideband hydrophone arrays of opportunity. Such arrays may be obtained by arranging together multiple smaller sub-arrays that were originally designed to work independently. The array of opportunity that results may be subject to practical mounting limitations, hence the typical constraint that closest array elements should not be spaced more than one half-wavelength may not be upheld. In these conditions, the array is affected by spatial ambiguity.**

**Our proposed scheme solves this issue by fusing direction-of-arrival information with side information on the estimated target location (obtained via multilateration). This makes it possible to eliminate most of the ambiguity, and yields accurate direction-of-arrival estimates. Our simulation results show that our scheme achieves satisfactory direction of arrival estimation and localization results. Moreover, even by relying on arrays of opportunity, we can outperform classical direction-of-arrival algorithms applied to larger arrays with half-wavelength spacing design.**

***Index Terms*—Wideband array processing; underwater acoustic signals; direction of arrival estimation; side information; multilateration; localization**

## I. Introduction

Stand-off monitoring and remote sensing are of great importance in many industrial, exploration, and environmental conservation scenarios. Common approaches for this challenging task include image- and video-based monitoring [1], LiDAR systems [2], as well as acoustic solutions [3]. In particular, non-invasive acoustic systems can help monitor key pelagic fish species in their natural habitat without harmful anthropogenic interference. For the cases where the accurate geolocation of sensed data is required, sonar systems usually employ hydrophone arrays engineered to provide the desired spatial scanning capabilities. Moreover, fusing the information from multiple arrays typically improves the performance of localization and ranging, even if the arrays are highly displaced and the received acoustic signals are not significantly correlated [4]. A particularly convenient case is represented by arrays whose elements can be extended modularly, achieving higher directivity and better output Signal-to-Noise Ratio (SNR) on demand. In order to avoid having to redesign an array from scratch, such extensions can also be achieved by "opportunistically" joining arrays that were originally designed to work independently. While some engineering issues may still appear, such as ensuring the synchronous sampling of all elements, the biggest challenge is that independent array modules may not be designed to be joined into a larger array. On the contrary, their physical design may give rise to different kinds of mounting issues. For example, a given minimum spacing among the sub-arrays may have to be ensured in order to preserve connectors, or to avoid that power and data cables bend in excess of their specifications.

There are at least two important consequences to these constraints. First, it may be impossible to construct typical array topologies such as uniform linear arrays (ULAs) or uniform rectangular arrays (URAs). Second, the maximum spacing of closest array elements may be forced to remain larger than $\lambda/2$, where $\lambda$ is the wavelength corresponding to the maximum operational acoustic frequency of the array's hydrophones. A larger spacing than $\lambda/2$ may lead to very significant ambiguities in beamforming and direction of arrival (DoA) estimation operations, which may not be removed by leveraging side physical characteristics of the array elements, such as a non-omnidirectional radiation pattern [5]. When the array is employed for localization purposes through multilateration, larger-than-$\lambda/2$ spacing may also lead to very significant errors [6].

Notably, most 3D wideband DoA estimation algorithms [5] work with predefined array shapes, or are limited to 2D, to specific signals, to a known number of objects to be found [7], or directly employ particle velocity sensors [8].

In this paper, we propose a wideband DoA estimation algorithm that works with generic 3D arrays with arbitrary element spacing. Our method hinges on the observation that most of the DoA ambiguity can be ruled out in case some further information about the target can be exploited. As we do not assume any cooperation with the target itself, we need to extract such additional information from additional array processing. Specifically, we estimate the location of the target through multilateration, using time difference of arrival (TDoA) measurements. This makes it possible to restrict the DoA search to an area around the actual location of the target, where ambiguity is mostly absent, even if the array elements are not sufficiently spaced to achieve high resolution [4], and the multilateration of the target is therefore not extremely accurate.

Our simulation results show that our algorithm effectively estimates DoAs and 3D target locations, making it possible to take advantage of multiple combined arrays, even when the resulting array topology is affected by sub-optimal spacing. Specifically, we show that stacking three 5-element pyramidal arrays (each of which could be, e.g., a separate USBL unit) into a 15-element array yields very good angle and localization

error performance. Moreover, our algorithm applied to such an array outperforms DoA estimation through a wideband delay-sum algorithm, even when the latter is applied to a properly designed cylindric array with 24 hydrophones.

In the remainder of this paper, we survey relevant related work (Section II), describe our DoA method (Section III), and provide performance results (Section IV). Finally, we draw concluding remarks in Section V.

## II. Related work

Array processing for underwater detection and communication has a long history, and includes contributions to sonar systems, communications and underwater target detection with passive and active arrays [9]. In recent times, classical beamforming algorithms have been mixed with different estimation or signal processing techniques in order to improve the accuracy and decrease the complexity of adaptive beamforming algorithms. For example, the work in [10] employs a particle filter to estimate the direction of arrival of an acoustic source. This is shown to improve the performance of Bartlett and conventional likelihood beamformers using real data from the SwellEx'96 experiment. By exploiting partial information related to the structure of a transmitted signal, the authors of [11] improve the performance of a blind DoA and channel parameter estimation algorithm from the literature [12].

To localize a blind node, [13] mixes DoA and time of flight (ToF) information related to the signals that the blind node receives from synchronous reference nodes. In pool experiments, the blind node integrates a 4-element linear array for DoA estimation. Tesei *et al.* [4] discuss sound source localization in 3D using one or two tetrahedral arrays deployed at different locations. Despite synchronous sampling in the two systems, no joint array processing is performed, as the distance between the arrays decorrelates the received signals.

Compressive sensing and sparse reconstruction techniques have also found application in underwater array processing. For example, the work in [14] relies on compressive beamforming to estimate the DoA of an underwater acoustic source via a forward-looking sonar transmitting continuous-wave comb signals. The system is proven using field experiment data. In [15] sparse reconstruction is used to detect the DoA of the sound emitted by underwater vessels using linear arrays. The authors carry out an experiment using a passive towed array sonar system to prove the performance of their algorithm. The work in [16] applies coherent signal subspace processing and compressive sensing to DoA estimation for wideband signals. The method yields higher resolution than the conventional minimum variance distortionless response (MVDR) beamformer.

As acoustic vector sensors already provide a first estimate of the direction of arrival of an underwater signal, several works involve one or more such sensors in DoA estimation tasks [17]–[19]. Arrays of vector sensors and coherent processing also improve the resolution of underwater DoA estimation for wideband coherent sources [20].

Wideband beamforming has recently spurred significant interest in the broadband terrestrial radio communication domain, and finds applications for underwater acoustic detection and communications as well. Liu and Weiss [5] provide an extensive coverage of classical approaches and recent research results for wideband array processing with applications to signal enhancement and DoA estimation. In the broadband underwater acoustic communication domain, [21] explores multichannel processing through diversity combining and optimal beamforming applied to the reception of high-speed underwater acoustic communication signals, and shows that the beamforming approach reduces the complexity of the receiver. The capability to coherently extract the energy of underwater multipath signal is demonstrated through a sea experiment. The work in [22] applies sparse Bayesian methods to estimate the DoA of wideband LFM signals using a uniform linear array. The fractional Fourier transform is employed to isolate the signal and improve the signal-to-reverberation and signal-to-noise ratios.

Typically, the development of signal processing algorithms for underwater acoustic arrays assumes a simple array topology, for which the steering vectors and array manifolds can be computed in close-form. Often, linear arrays are used [10], [11], [13]–[15]. A study involving 3D, 4-element tetrahedral arrays is provided in [4]. Unlike the above literature, in this paper we propose a DoA estimation algorithm that works on arbitrary, 3D underwater array topologies, as we typically obtain by combining multiple sub-arrays originally conceived as independent units. In doing so, we assume that we cannot rely on properly spaced array elements (i.e., we need to deal with the ambiguity arising from larger-than-$\lambda/2$ spacing), and target wideband array processing. Note that, unlike in [4], we synchronously sample and jointly process all array elements. The next section describes our approach.

## III. Wideband DoA estimation algorithm

### A. Key idea

We assume to employ an array of wideband hydrophones arranged into a known topology. We assume these elements to be comparatively close and sampled synchronously, but not necessarily spaced to obey the $\lambda/2$ constraint. The array is co-located with a projector that transmits wideband signals, such as linear chirps of duration $T$, spanning the frequencies from $f_{\min}$ to $f_{\max}$. The task of the array is to detect the DoA of the signal reflections off targets in the surrounding areas. As the suboptimal spacing of the array elements leads to ambiguity in DoA estimation, our algorithm mitigates such ambiguity by fusing the output of delay-sum wideband array processing with the outcome of TDoA-based multilateration.

### B. Algorithm description

Call the transmitted chirp

$$f(t) = \cos\left(2\pi \, \frac{f_{\max} - f_{\min}}{2T} \, t^2 + f_{\min} \, t\right), \qquad (1)$$

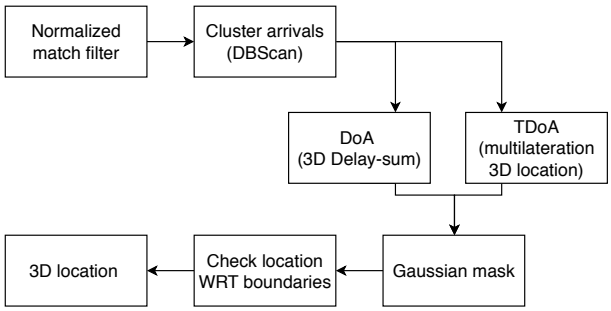


Fig. 1. Flow diagram of the DoA estimation and localization algorithm.

and let $s_n(t)$ be the real-valued signal received by the $n$th array element. With reference to Fig. 1, our scheme proceeds by first detecting $f(t)$ within the $s_n(t)$ signals using a normalized matched filter. For each array element, the output of the filter is expressed as

$$R_n(\tau) = \frac{\displaystyle\int_0^{+\infty} f(t)\, s_n(t+\tau)\,\mathrm{d}t}{\left(\displaystyle\int_0^{T} s_n^2(t)\,\mathrm{d}t \int_0^{+\infty} f^2(t)\,\mathrm{d}t\right)^{1/2}}\,. \tag{2}$$

We search relevant cross-correlation peaks in $R_n(\tau)$ via a sliding window method. In more detail, we consider a window of length $T$ aligned with the beginning of $R_n(\tau)$, and take the highest peak in the window; then we slide the window, take the highest peak and repeat the process until the window has reached the end of $R_n(\tau)$. The result of this process is a reduction of the peaks in $R_n(\tau)$, whereby secondary peaks that are never the tallest in any window are discarded. Call $\mathcal{P}_n$ the set of peaks thus singled out, where a peak $p \in \mathcal{P}_n$ is fully defined by its time of occurrence $t$, its amplitude $a$ and the hydrophone $n$ that detects it, i.e., $p = (t, a, n) \in \mathcal{P}_n$.

We proceed by applying the DBScan algorithm [23] over the whole set of peaks

$$\mathcal{P} = \mathcal{P}_1 \cup \cdots \cup \mathcal{P}_n\,. \tag{3}$$

DBScan corresponds to a function

$$\mathcal{C} = \mathcal{D}(\mathcal{P}) \tag{4}$$

that returns a number of subsets of arrivals $C \in \mathcal{C}$, such that ideally a subset $C$ contains groups of detections that correspond to the same target. The algorithm is configured to seek arrivals detected by at least 50% of the array elements, and spaced in time no more than the maximum propagation delay difference between any two elements. This step serves as a very fast "coherence test," and enables our algorithm to discard peaks that are not detected reliably by all elements, or that are overly spaced in time, and thus unlikely to correspond to the same signal reflection from a nearby target. Note that, in general, a cluster $C$ may contain peaks from only a subset of the array elements, as some may be shadowed by other hydrophones.

We now consider a set of elevation angles $\Theta$ and azimuth angles $\Phi$, and scan the power received by the array along every direction identified by a pair $(\theta, \phi)$, for $\theta \in \Theta$ and $\phi \in \Phi$. Specifically, for each cluster $C$, we measure the energy perceived by the array along different directions through a wideband delay-sum algorithm [5]. We implement the algorithm by computing a 1024-point fast Fourier transform (FFT) of the signal portion that covers the arrivals in $C$ in each hydrophone. We then apply a different, frequency-dependent phase shift vector to each frequency bin in order to steer the array towards the direction $(\theta, \phi)$. Finally, we convert back to the time domain via an inverse FFT operation, and sum the resulting outputs across all hydrophones. The outcome of the wideband delay-sum algorithm is a map $\alpha(\theta, \phi)$ of the power received over all scanning directions specified by sets $\Theta$ and $\Phi$. As we consider arrays of opportunity where the elements may be spaced more than $\lambda/2$, the delay-sum map may be affected by ambiguities, and may indicate the reception of a significant amount of power from directions different than the true target direction.

In order to reduce such ambiguity, we filter out irrelevant peaks using side TDoA information. In more detail, call $\mathbf{u} = [x \;\; y \;\; z]^\mathsf{T}$ the Cartesian coordinates of the target, $\mathbf{u}_n = [x_n \; y_n \; z_n]^\mathsf{T}$ the location of hydrophone $n$, and $t_0$ the time of the earliest across all peaks in cluster $C$. Without loss of generality, assign index 0 to the hydrophone that receives this arrival. Finally, call $c$ the sound speed near the array, which we assume to be known. For each peak $p = (t, a, n) \in C$, the corresponding multilateration equation is

$$x \cdot X_n + y \cdot Y_n + z \cdot Z_n + D_n = 0\,, \tag{5}$$

where

$$X_n = \frac{2x_n}{c\,t} - \frac{2x_0}{c\,t_0} \tag{6}$$

(analogous equations can be written for $Y_n$ and $Z_n$), and

$$D_n = c\,(t - t_0) - \frac{x_n^2 + y_n^2 + z_n^2}{c\,t} + \frac{x_0^2 + y_0^2 + z_0^2}{c\,t_0}\,. \tag{7}$$

Collecting one equation such as (5) for every peak in cluster $C$ results in an over-determined system of equations, which we solve through Moore-Penrose's pseudo-inverse. The result is a rough estimate of the target location $\mathbf{u}^\star = [x^\star \; y^\star \; z^\star]^\mathsf{T}$, which can be converted in polar coordinates to yield

$$\mathbf{u}^\star = [r^\star \; \theta^\star \; \phi^\star]^\mathsf{T}\,. \tag{8}$$

We exploit the above estimate to define a masking function having the shape of a truncated bi-variate Gaussian kernel

$$m(\theta, \phi) = \min\left\{1;\; \frac{1}{2\pi\sigma_\theta\sigma_\phi}\, \mathrm{e}^{-\frac{(\theta-\theta^\star)^2}{2\sigma_\theta^2}}\, \mathrm{e}^{-\frac{(\phi-\phi^\star)^2}{2\sigma_\theta^2}}\right\}, \tag{9}$$

where $\sigma_\theta = \pi/8$ and $\sigma_\phi = \pi/4$. Using $m(\theta, \phi)$, we mask the output of the wideband delay-sum beamformer in order to mitigate (and typically fully remove) ambiguities. Finally, we set the estimated DoA for the received signal as

$$\alpha^\star = \arg\max_{\theta,\phi}\, \alpha(\theta, \phi)\, m(\theta, \phi)\,. \tag{10}$$

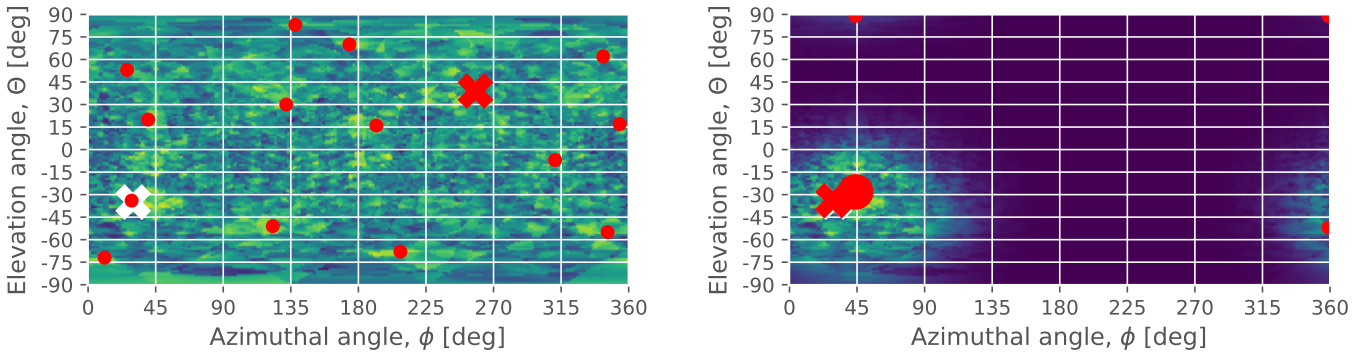


Fig. 2. Intensity map at the output of the wideband delay-sum beamformer without (left) and with (right) TDoA multilateration-based masking. The latter mitigates the ambiguity and makes it possible to correctly estimate the location of the target (white cross). Yellow hues denote a stronger signal.

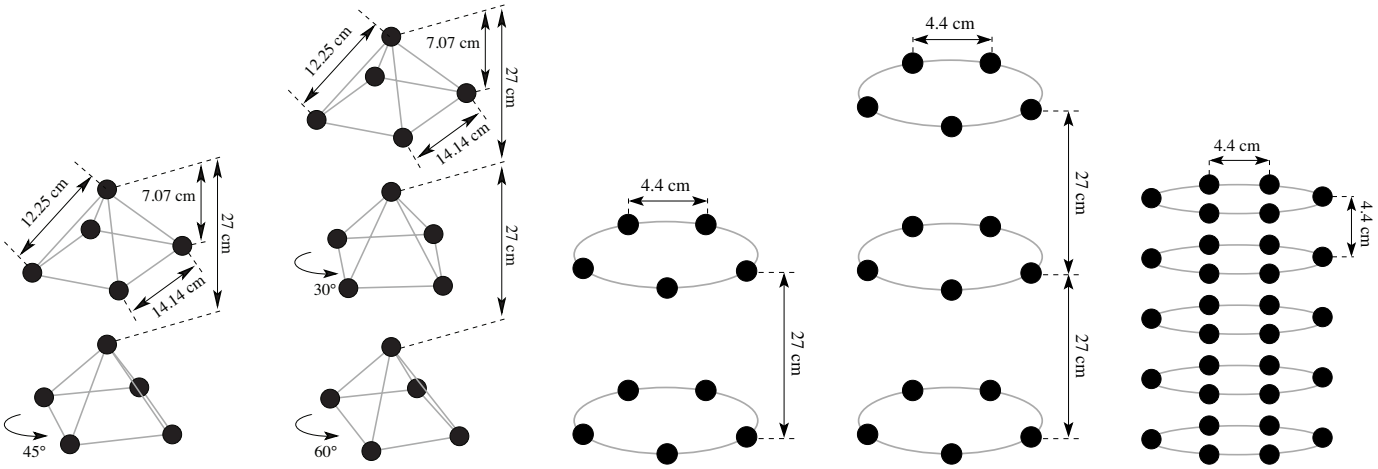


(a) Array 1 (b) Array 2 (c) Array 3 (d) Array 4 (e) Array 5

Fig. 3. Array topologies considered in this paper.

Fig. 2 provides an example of the delay-sum output (left panel). Here, several local maxima exist (red dots), and noise easily leads to a wrong estimate (red cross) of the target's DoA (white cross). Conversely, applying the multilateration-based mask (right panel) singles out the target's location and enables accurate DoA estimation. We note that some local maxima still remain even after applying the mask, but these are now sufficiently mitigated, and do not impede a correct DoA estimation.

As a final step, the estimated DoA is fused with ranging information and passed on as a valid output only if the target is found to be located within the boundaries of the water column.

## IV. Performance Evaluation

To illustrate the performance of our DoA estimation algorithm, we assume that the signals transmitted to detect targets in the proximity of our arrays of opportunity is a linear chirp of duration $T = 10$ ms and spanning the acoustic band from $f_{\min} = 7$ kHz to $f_{\max} = 17$ kHz.

We consider five different arrays, as illustrated in Fig. 3. *Array 1* is composed of two 5-element pyramidal arrays having a base side length of 14.14 cm and an height of 7.07 cm. The sub-arrays are stacked at a distance of 27 cm, and the bottom one is rotated by 45°. This is typical in the case each sub-array is, e.g., a separate USBL unit, whose connector mounting and cable bending constraints impede placing the units closer than a given maximum distance. *Array 2* is similar to array 1, but is composed of three pyramidal arrays stacked at a distance of 27 cm. In this case, the second array is rotated by 30° and the third by 60°. *Array 3* is composed of two circular sub-arrays of radius 3.5 cm, placed at a distance of 27 cm from each other. Each sub-array embeds 5 elements (the same as a pyramidal array). The elements are equally spaced along the circumference and closest elements are 4.4 cm apart. *Array 4* is similar to array 3, but is composed of three rather than two circular sub-arrays. Finally, *Array 5* is a cylindric array composed of 4 circular sub-arrays of 6 elements each. The distance between closest elements along the same circle and across different circles is 4.4 cm. We remark that assuming a sound speed of 1500 m/s, such a distance corresponds to $\lambda/2$ spacing up to a frequency of $\approx$ 17 kHz. Because array 5 is designed with proper $\lambda/2$ spacing throughout all frequencies

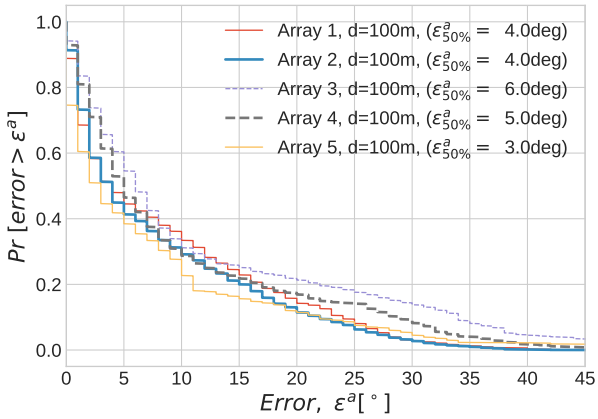


Fig. 4. CCDF of the azimuthal angle estimation error for a target located at 100 m from the array.

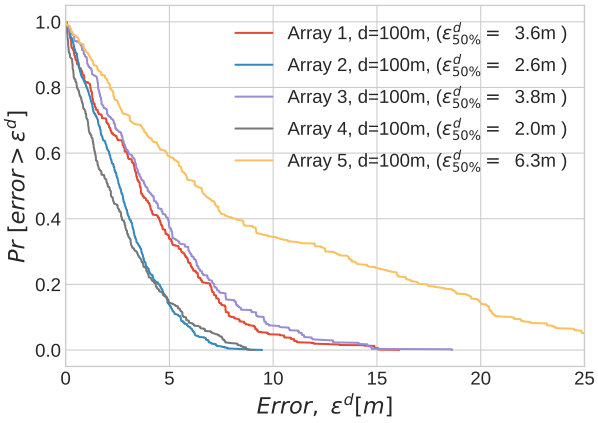


Fig. 5. CCDF of the depth estimation error for a target located at 100 m from the array.

spanned by the chirp signal, we do not apply the $m(\theta, \phi)$ mask to the wideband delay-sum output in this case.

To simulate our algorithm, we consider an isovelocity water body of depth 100 m. We position the array of opportunity at a depth of 10 m, and place a target at a distance of either 100 m or 200 m from the array, at different azimuthal angles $\phi$ and depths $d$. We simulate acoustic propagation in this environment by considering the three strongest paths that would be detected by the array, namely the specular path and first-order reflections off the sea surface and bottom. We neglect second-order reflections, which anyway would be comparatively less powerful, given that they originate from a target-reflected signal. We simulate our DoA estimation and localization scheme over a Monte-Carlo set of 270 target locations, chosen at random to be representative of all array lookout directions. For each location, we repeat the estimation for 10 different noise realizations. We consider a SNR of $-10$ dB.

For a target located at a distance of 100 m, Fig. 4 shows the complementary cumulative distribution function (CCDF) of the azimuthal angle estimation error for the five array types discussed above. We observe that arrays 1 to 4 perform equivalently. Array 2 achieves a marginally but noticeably lower angle estimation error than array 1, because its 5-element pyramidal arrays are rotated by $30°$ and $60°$, respectively, which yields a better discrimination capability over the azimuthal plane. Array 5 provides the best performance among the considered arrays (median error of about $3°$). This is due both to the larger number of elements in each circular section of the array and to the denser spacing of the hydrophones, which respect the $\lambda/2$ constraint for all frequencies in the 7–17 kHz band.

We now consider the capability of the array to correctly estimate the depth of the target. Fig. 5 shows the CCDF of the depth estimation error. We observe that taller arrays yield better results: arrays 2 and 4 achieve a better depth estimation error than arrays 1 and 3 (specifically, a median error of up to 2.6 m, against up to 3.8 m for arrays 1 and 3). We remark that the arrangement of the sub-arrays is comparatively less important for depth estimation. In fact, pyramidal and circular sub-arrays yield similar results because the distance between subsequent sub-arrays is 27 cm in all cases. Array 5 provides the worst performance: we recall that since the elements of array 5 are properly spaced, we do not apply TDoA-based masking to the delay-sum output for Array 5, resulting in a higher median depth estimation error of about 6.3 m.

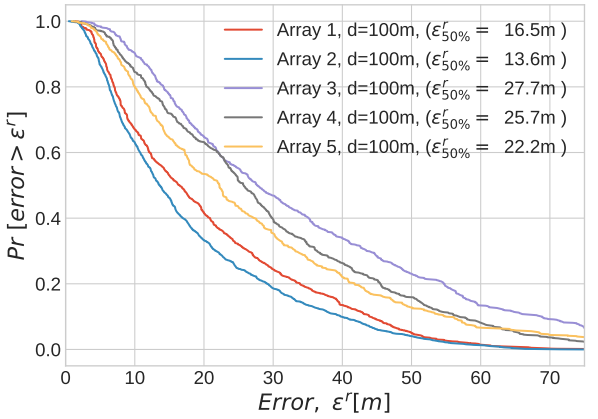


Fig. 6. CCDF of the location error for a target located at 100 m from the array.

Angle and depth information can be combined with measurements of the transmitted signal's round-trip time in order to yield an estimate of the 3D target location. Fig. 6 shows the CCDF of the target location error. We observe that arrays 1 and 2 achieve the best performance, with slightly better results for array 2 due to its higher number of elements and larger height. Arrays 3 and 4 achieve the worst performance (with array 4 slightly better than array 3 due again to the larger height and number of elements). Array 5 ranks intermediately,

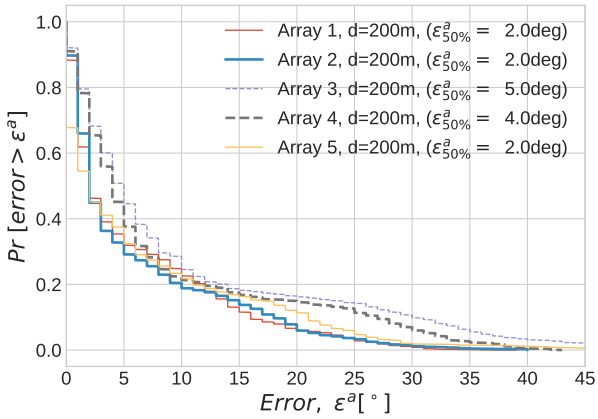


Fig. 7. CCDF of the azimuthal angle estimation error for a target located at 200 m from the array.

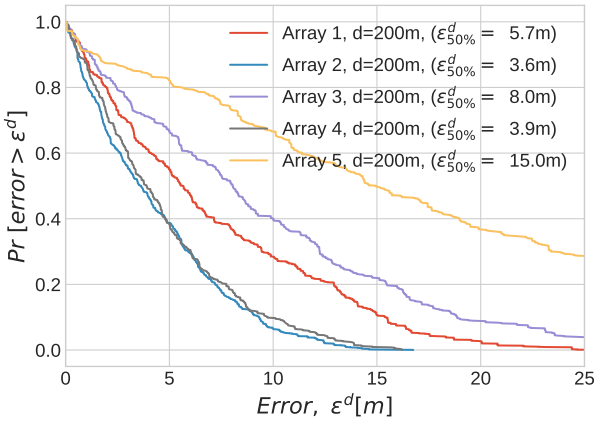


Fig. 8. CCDF of the depth estimation error for a target located at 200 m from the array.

with a good median error, but higher worst-case and best-case errors. The best median error is achieved by Array 2 (13.6 m).

When the target is 200 m away from the array, the depth estimation and localization performance change slightly. Fig. 7 confirms the intuition that the distance of the target does not significantly influence the azimuthal angle error. The performance of all arrays is very good, with median errors not exceeding $5°$, and 80% of the errors being less than $15°$. The depth estimation error (Fig. 8) is expectedly worse than in the 100 m-distance case, because the same elevation angle estimation error translates into larger depth discrepancies if the target is farther. In any event, arrays 2 and 4 still achieve the best error performance (with a median error less than 4 m); arrays 1 and 3 achieve a median error of 5.7 m and 8 m, respectively. The limited vertical extension of array 5 and the lack of TDoA-based masking compound to yield the worst depth estimation performance, with a median error of 15 m.

Finally, we show the overall localization error in Fig. 9. The trend and ranking of the algorithms is the same as in Fig. 6: arrays 2 and 4 achieve the lowest error, whereas arrays 1, 3 and 5 show worse performance. In the best case of array 2, the median error is less than 20 m, and 80% of the estimates are affected by an error of less than 50 m.

From the above results, we conclude that the triple pyramidal structure of array 2 yields the best tradeoff between azimuthal and elevation angle estimation capabilities, provided that the ambiguity arising from the spacing larger than $\lambda/2$ is corrected through side information, as is the case for our TDoA-based mask. More broadly, we also conclude that our algorithm is a promising solution to achieve satisfactory array performance when multiple smaller sub-arrays are opportunistically combined into a larger array.

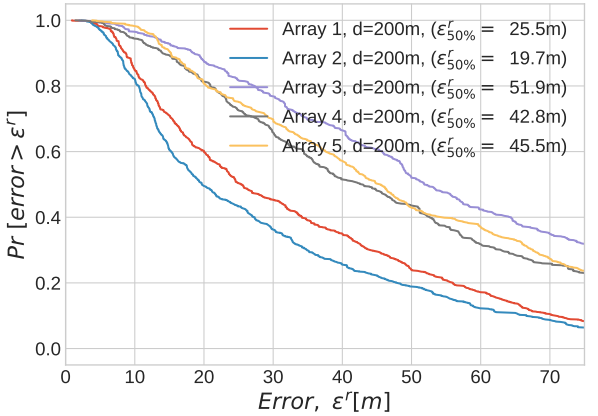


Fig. 9. CCDF of the location error for a target located at 200 m from the array.

## V. Conclusions

We present a wideband DoA estimation algorithm designed to operate with sub-optimally designed acoustic arrays. Such arrays may result from the opportunistic combination of smaller, typically independent sub-arrays into a bigger structure, with non-ideal element spacing possibly exceeding the $\lambda/2$ constraint. We proposed to solve the spatial ambiguity issues that affect such arrays by augmenting a delay-sum DoA estimation algorithm with a multilateration step: we estimate the location of the target from TDoA information, and mask the delay-sum output to significantly mitigate the ambiguity.

Our results show that the proposed scheme yields satisfactory azimuthal angle and depth estimation error, and therefore good 3D localization results. For a specific 15-element array composed of three-pyramidal sub-arrays, we show that our method outperforms classical DoA estimation applied to a 24-element cylindric array, whose element spacing is less than or equal to $\lambda/2$ throughout the acoustic band of interest. Future work includes the evaluation of our algorithm in a sea trial.

## Acknowledgment

This work has received support from the European Union's Horizon 2020 Research and Innovation Programme under grant agreement no. 773753 (SYMBIOSIS).

## REFERENCES


[1] D. Levy, Y. Belfer, E. Osherov, E. Bigal, A. P. Scheinin, H. Nativ, D. Tchernov, and T. Treibitz, "Automated analysis of marine video with limited data," in *Proc. IEEE/CVF CVPRW*, 2018.

[2] E. Dubrovinskaya, F. Dalgleish, B. Ouyang, and P. Casari, "Underwater LiDAR signal processing for enhanced detection and localization of marine life," in *Proc. MTS/IEEE OCEANS*, 2018.

[3] L. Paull, S. Saeedi, M. Seto, and H. Li, "AUV navigation and localization: A review," *IEEE Journal of Oceanic Engineering*, vol. 39, no. 1, pp. 131–149, 2014.

[4] A. Tesei, S. Fioravanti, V. Grandi, P. Guerrini, and A. Maguer, "Localization of small surface vessels through acoustic data fusion of two tetrahedralarrays of hydrophones," in *Proc. ECUA*, Jul. 2012.

[5] W. Liu and S. Weiss, *Wideband beamforming: concepts and techniques*. John Wiley & Sons, Mar. 2010.

[6] S. Stergiopoulos, *Advanced signal processing handbook: theory and implementation for radar, sonar, and medical imaging real time systems*. CRC press, 2018.

[7] F. Andersson, M. Carlsson, J.-Y. Tourneret, and H. Wendt, "A method for 3D direction of arrival estimation for general arrays using multiple frequencies," in *Proc. CAMSAP*, 2015.

[8] K. T. Wong and M. D. Zoltowski, "Closed-form underwater acoustic direction-finding with arbitrarily spaced vector hydrophones at unknown locations," *IEEE J. Ocean. Eng.*, vol. 22, no. 3, pp. 566–575, 1997.

[9] R. J. Vaccaro, "The past, present, and the future of underwater acoustic signal processing," *IEEE Signal Process. Mag.*, vol. 15, no. 4, pp. 21–51, Jul. 1998.

[10] X. Zhong, A. B. Premkumar, and W. Wang, "Direction of arrival tracking of an underwater acoustic source using particle filtering: Real data experiments," in *Proc. IEEE Tencon–Spring*, Apr. 2013, pp. 420–424.

[11] W. Chen, T. Luo, F. Chen, F. Ji, and H. Yu, "Directions of arrival and channel parameters estimation in multipath underwater environment," in *Proc. MTS/IEEE OCEANS*, Apr. 2016, pp. 1–4.

[12] H. Amindavar and A. M. Reza, "A new simultaneous estimation of directions of arrival and channel parameters in a multipath environment," *IEEE Trans. Signal Process.*, vol. 53, no. 2, pp. 471–483, Feb. 2005.

[13] W. A. P. van Kleunen, K. C. H. Blom, N. Meratnia, A. B. J. Kokkeler, P. J. M. Havinga, and G. J. M. Smit, "Underwater localization by combining time-of-flight and direction-of-arrival," in *Proc. MTS/IEEE OCEANS*, Apr. 2014, pp. 1–6.

[14] H. Song, J. Qin, C. Yang, and M. Diao, "Compressive beamforming for underwater acoustic source direction-of-arrival estimation," in *Proc. IEEE ICCE-TW*, May 2018.

[15] M. R. Devi, N. S. Kumar, and J. Joseph, "Sparse reconstruction based direction of arrival estimation of underwater targets," in *Proc. SYMPOL*, Nov. 2015, pp. 1–6.

[16] J. Li, Q.-h. Lin, C.-y. Kang, K. Wang, and X.-T. Yang, "DoA estimation for underwater wideband weak targets based on coherent signal subspace and compressed sensing," *MDPI Sensors*, vol. 18, no. 3, Mar. 2018.

[17] A. Abdi, H. Guo, and P. Sutthiwan, "A new vector sensor receiver for underwater acoustic communication," in *Proc. MTS/IEEE OCEANS*, Sep. 2007, pp. 1–10.

[18] T. Zhao, H. Chen, H. Zhang, Z. Li, and L. Tong, "Design of underwater particle velocity pickup sensor," in *Proc. IEEE/OES CO*A, Jan. 2016, pp. 1–6.

[19] J. Cao, J. Liu, J. Wang, and X. Lai, "Acoustic vector sensor: reviews and future perspectives," *IET Signal Processing*, vol. 11, no. 1, pp. 1–9, 2017.

[20] G. Sun, J. Hui, and Y. Chen, "Fast direction of arrival algorithm based on vector-sensor arrays using wideband sources," *Springer J. Marine. Sci. Appl.*, vol. 7, pp. 195–199, Sep. 2008.

[21] M. Stojanovic, J. A. Catipovic, and J. G. Proakis, "Reducedcomplexity spatial and temporal processing of underwater acoustic communication signals," *J. Acoust. Soc. Am.*, vol. 98, no. 2, pp. 961–972, 1995.

[22] X. Li, H. Jia, and M. Yang, "Underwater target detection based on fourth-order cumulant beamforming," *ASA Proc. of Meetings on Acoustics*, vol. 31, no. 1, pp. 1–9, 2017.

[23] M. Ester, H.-P. Kriegel, J. Sander, and X. Xu, "A density-based algorithm for discovering clusters in large spatial databases with noise," in *Proc. AAAI KDD*, vol. 96, no. 34, 1996, pp. 226–231.